

FLYWHEEL ZERO-BIAS AMB SYSTEM WITH FORCE BASE SWITCHING SERVO BACKSTEPPING CONTROL

Selim Sivrioglu

Department of Energy Systems
Gebze Institute of Technology
Gebze 41400, Turkey
s.selim@gyte.edu.tr

Kenzo Nonami

Department of Electronics and
Mechanical Engineering
Chiba University, Japan.
nonami@faculty.chiba-u.jp

ABSTRACT

This study presents a control design approach for a zero bias active magnetic bearing system. A nonlinear control approach based on a control current switching rule is studied experimentally for an energy storage flywheel active magnetic bearing (AMB) system. The equation of motion for the rigid rotor-AMB system is transformed to have a decentralized structure for the control design. To compute nonlinear control currents, a servo backstepping control is designed for each axis of the AMB. The proposed approach is experimentally verified using a high speed digital signal processor (DSP).

INTRODUCTION

The use of active magnetic bearings in flywheel energy storage systems is a promising research field due to the significant advantages of AMB's such as contactless and frictionless very high speed rotation [1]-[3]. Besides such great advantages, in reality, the competitiveness of the magnetic bearings to other mechanical bearings in flywheel applications depends strongly on the reduction in bearing losses. Conventional active magnetic bearings use linearizing bias currents with superposed control currents to obtain a linear characteristic of the magnetic actuator. The bias currents become the main source of the bearing losses. Zero-bias active magnetic bearings have potential to realize reduction in bearing losses.

Nonlinear control of active magnetic bearings has been previously studied using different control approaches [4]-[5]. Zero-bias control of active magnetic bearing have also been studied [6]-[8]. In this study, as a continuation of the previous works, an experimental approach is realized for a specific flywheel AMB system. For this aim, a nonlinear control structure is first defined for a single axis magnetic bearing. Then, a flywheel (AMB) test system is introduced and modeled with a decentralization approach. Finally, experimen-

tal verification is realized and results are presented.

FORCE BASE SWITCHING

A single axis rotor-magnetic bearing system depicted in Figure 1 is used to illustrate the proposed control structure. The equation of motion for the rotor-active magnetic bearing system shown in Fig.1 is simply derived as

$$M\ddot{x} = \bar{f} \quad (1)$$

where M is the mass of the rotor and \bar{f} is the electromagnetic force produced by a magnetic actuator. The actuator is composed of a pair of electromagnets; one is located at $x > 0$ and the other at $x < 0$ side. Note that each electromagnet generates attractive force. The resulting force acting on the rotor is given by

$$\begin{aligned} \bar{f} &= \bar{f}_1 - \bar{f}_2 \\ &= \frac{K_a \bar{i}_1^2}{(X_0 - x)^2} - \frac{K_a \bar{i}_2^2}{(X_0 + x)^2} \end{aligned} \quad (2)$$

where K_a and X_0 denote the magnetic force coefficient and the air gap between rotor and magnet, respectively. Using the variable transformation $x_1 = x$, $x_2 = \dot{x}$, the second order control system is obtained as

$$\begin{aligned} \dot{x}_1 &= x_2 \\ \dot{x}_2 &= \bar{b}\bar{f} \\ y &= x_1 \end{aligned} \quad (3)$$

where y denotes the measured output of the system and $\bar{b} = 1/M$. In reality, each electromagnet is driven by the control currents \bar{i}_1 and \bar{i}_2 to produce control forces \bar{f}_1 and \bar{f}_2 . As is well known, the aim of the control in a rotor magnetic bearing system is to suspend the rotor in the center line in presence of disturbances. To realize this objective a controller is necessary to generate the electromagnetic control forces for any rotor position. Therefore when the control forces are known, the

currents are derived from these forces. An important property of the proposed control structure is only one electromagnet in each axis of the active magnetic bearing has a current flow at any given time. A switching rule is necessary to realize the proposed control structure. The control currents of the electromagnets may be switched depending on the rotor displacement. However, in displacement base switching, positiveness of the square root in control current equation is not guaranteed due to dependence of control force to both displacement and velocity. In this study, it is proposed to switch the control currents according to the sign of the control force \bar{f} such as

$$\begin{aligned} \bar{f} \geq 0, \quad \bar{f}_2 = 0, \quad \bar{f}_1 = \bar{f}, \quad \bar{i}_1 &= (X_0 - x) \sqrt{\frac{\bar{f}_1}{K_a}} \\ \bar{f} < 0, \quad \bar{f}_1 = 0, \quad \bar{f}_2 = -\bar{f}, \quad \bar{i}_2 &= (X_0 + x) \sqrt{\frac{\bar{f}_2}{K_a}} \end{aligned} \quad (4)$$

Note that the square root yields always a real number in the above computations.

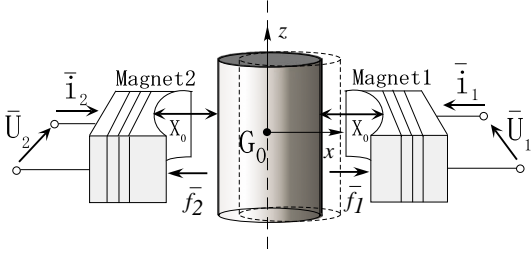


FIGURE 1: A single axis rotor-magnetic bearing

MODELING OF FLYWHEEL-AMB SYSTEM

Equations of Motion

The flywheel-AMB system depicted in Figure 2 shows the rotor and placement of the magnetic actuators in upper and lower locations in xGz plane. Note that four other magnetic actuators are also placed in yGz plane symmetrically, but are not shown in the Figure 2. The equation of motion of the rigid rotor-active magnetic bearing system is derived as

$$\begin{aligned} M\ddot{x}_g &= (f_1 - f_3) + (f_5 - f_7) \\ I_r\ddot{\theta}_y &= -(f_1 - f_3)L_u - (f_5 - f_7)L_l \\ M\ddot{y}_g &= (f_2 - f_4) + (f_6 - f_8) \\ I_r\ddot{\theta}_x &= (f_2 - f_4)L_u + (f_6 - f_8)L_l \end{aligned} \quad (5)$$

where x_g and y_g denote the displacement of the rotor's center of mass. Similarly, θ_y and θ_x are the angular displacement of the rotor around the x and y axes. $f_1, f_2, f_3,$ and f_4 denote the electromagnetic forces for the upper bearing in the x and y

directions. Similarly, $f_5, f_6, f_7,$ and f_8 show the electromagnetic forces for the lower bearing. The upper and lower bearing forces in the x direction are given as

$$\begin{aligned} f_1 &= \frac{K_u i_1^2}{(X_0 - x_u)^2} & f_3 &= \frac{K_u i_3^2}{(X_0 + x_u)^2} \\ f_5 &= \frac{K_l i_5^2}{(X_0 - x_l)^2} & f_7 &= \frac{K_l i_7^2}{(X_0 + x_l)^2} \end{aligned} \quad (6)$$

The electromagnetic forces for the y direction have the same form.

Decentralization of Upper and Lower AMB

The equations of motion obtained in (5) are derived according to the movement of the rotor's center of mass. On the other hand, the measured signals are the displacements of the rotor at the lower and upper sensor locations. Since sensor locations are distinct from the mass center, the computation of the displacements of the rotor's center of mass and angular displacements are necessary during control operation. Instead of computing the displacements x_g, y_g, θ_y and θ_x , the computation of the displacements of the rotor at the magnet locations makes the control system collocated. To this aim, the equations of the rotor AMB system may be transformed to the actuator locations. The displacement at the upper AMB location for the x direction is obtained as

$$x_u = x_g - L_u \theta_y \quad (7)$$

Taking the double derivative of the above equation and substituting Equations (5) and (6) into the obtained derivations, the equations are derived as

$$\begin{aligned} \ddot{x}_u &= \ddot{x}_g - L_u \ddot{\theta}_y = \frac{1}{M} f_1 - \frac{1}{M} f_3 \\ &\quad - L_u \left(-\frac{1}{I_r} f_1 L_u + \frac{1}{I_r} f_3 L_u \right) \\ \ddot{x}_u &= a_u \left[\frac{K_u i_1^2}{(X_0 - x_u)^2} - \frac{K_u i_3^2}{(X_0 + x_u)^2} \right] \end{aligned} \quad (8)$$

where

$$a_u = \left(\frac{1}{M} + \frac{L_u^2}{I_r} \right) \quad (9)$$

The transformation of the equations for the location of lower AMB is realized with the same derivation procedure and follows as

$$\begin{aligned} x_l &= x_g - L_l \theta_y \\ \ddot{x}_l &= \ddot{x}_g - L_l \ddot{\theta}_y = \frac{1}{M} f_5 - \frac{1}{M} f_7 \\ &\quad - L_l \left(-\frac{1}{I_r} f_5 L_l + \frac{1}{I_r} f_7 L_l \right) \\ \ddot{x}_l &= a_l \left[\frac{K_l i_5^2}{(X_0 - x_l)^2} - \frac{K_l i_7^2}{(X_0 + x_l)^2} \right] \end{aligned} \quad (10)$$

where

$$a_l = \left(\frac{1}{M} + \frac{L_l^2}{I_r} \right) \quad (11)$$

Note that in the above derivation process only the forces that directly effect the considered points are taken into account. When the transformation is done for the upper actuator location (x_u, y_u) on the rotor, the upper AMB forces f_1 and f_3 are considered and f_5, f_7 are taken as zero. For the lower actuator location (x_l, y_l) , the forces f_5 and f_7 are assumed to be effective and f_1, f_3 are taken as zero. Similarly, the displacement in the y direction is given as

$$\begin{aligned} y_u &= y_g + L_u \theta_x \\ y_l &= y_g + L_l \theta_x \end{aligned} \quad (12)$$

Repeating the same procedure, the transformed equations are derived as

$$\begin{aligned} \ddot{y}_u &= a_u \left[\frac{K_u i_2^2}{(Y_0 - y_u)^2} - \frac{K_u i_4^2}{(Y_0 + y_u)^2} \right] \\ \ddot{y}_l &= a_l \left[\frac{K_l i_6^2}{(Y_0 - y_l)^2} - \frac{K_l i_8^2}{(Y_0 + y_l)^2} \right] \end{aligned} \quad (13)$$

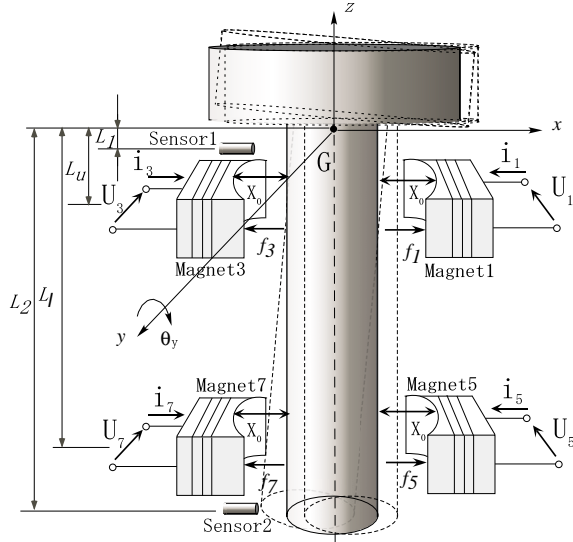


FIGURE 2: Flywheel-AMB systems

CONTROL DESIGN

Servo Control Structure

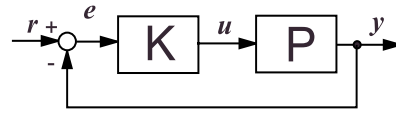
The standard backstepping design which uses the control structure shown in Figure 3(a) does not include any integral action in control input. In a controller, integral part makes the steady-state error zero with increasing of time. Therefore, an integral part will be added artificially as depicted in

Figure 3(b). Since each axis became independent of each other after the transformation of the equations to actuator locations, the design of the nonlinear zero-bias control may be defined only for one axis. To this aim, the system equation obtained in equation (8) for upper AMB may be written as follows

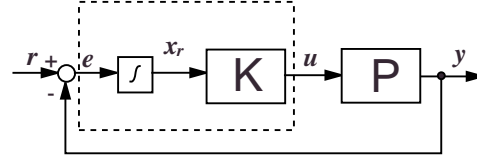
$$\begin{aligned} \dot{x}_r &= e \\ \dot{e} &= \dot{r} - \dot{x}_u \\ \dot{x}_u &= a_u f \\ y &= x_u \end{aligned} \quad (14)$$

Using the variable transformations $r = 0, x_1 = x_r, x_2 = x_u, x_3 = \dot{x}_u$, the control system is written as

$$\begin{aligned} \dot{x}_1 &= x_2 \\ \dot{x}_2 &= x_3 \\ \dot{x}_3 &= a_u f \\ y &= x_2 \end{aligned} \quad (15)$$



(a)



(b)

FIGURE 3: Servo control system structure (a) without integral (b) with integral

Backstepping Procedure

Since the control system given in equation (15) is third-order, the controller will be developed in three steps. In backstepping, error variables are defined in each step and stability of the control system is satisfied by control Lyapunov functions.

Step 1.

Suppose the output error variable z_1 is defined as:

$$z_1 = y - y_d \quad (16)$$

where y_d is the desired value of the output y . Deriving z_1 with respect to time such as

$$\begin{aligned} \dot{z}_1 &= \dot{x}_1 - \dot{y}_d \\ &= x_2 \end{aligned} \quad (17)$$

Note that derivative of the desired value y_d becomes zero due to its constant value. In equation

(17), x_2 behaves as a virtual control input. Defining a new error variable to eliminate x_2 such as

$$z_2 = x_2 - \alpha_1(x_1) \quad (18)$$

Using equation (18), the derivative of z_1 becomes

$$\dot{z}_1 = z_2 + \alpha_1(x_1) \quad (19)$$

Here $\alpha_1(x_1)$ represents the stabilizing function. Suppose a candidate Lyapunov function is defined as

$$V_1 = \frac{1}{2}z_1^2 \quad (20)$$

Taking the derivative of V_1 , one can get

$$\begin{aligned} \dot{V}_1 &= z_1 \dot{z}_1 \\ &= z_1[z_2 + \alpha_1(x_1)] \end{aligned} \quad (21)$$

Selecting the stabilizing function as follows:

$$\alpha_1(x_1) = -c_1 z_1 \quad (22)$$

where $c_1 > 0$. The derivative \dot{V}_1 becomes

$$\dot{V}_1 = -c_1 z_1^2 + z_1 z_2 \quad (23)$$

As is seen above, a global stability condition is not satisfied since $z_1 z_2$ term exists.

Step 2.

In this step, the behavior of error variable z_2 will be investigated. First, time-derivation of z_2 is

$$\begin{aligned} \dot{z}_2 &= \dot{x}_2 - \dot{\alpha}_1(x_1) \\ &= x_3 + c_1 x_2 \end{aligned} \quad (24)$$

To eliminate x_3 in above equation, a new error variable z_3 is defined as

$$z_3 = x_3 - \alpha_2(x_1, x_2) \quad (25)$$

Now, the derivative of z_2 becomes

$$\dot{z}_2 = z_3 + \alpha_2(x_1, x_2) + c_1 x_2 \quad (26)$$

With the extension of error variables, a new Lyapunov function is defined as

$$V_2 = V_1 + \frac{1}{2}z_2^2 \quad (27)$$

The time-derivative of V_2 is

$$\begin{aligned} \dot{V}_2 &= \dot{V}_1 + z_2 \dot{z}_2 \\ &= -c_1 z_1^2 + z_1 z_2 + z_2[z_3 + \alpha_2(x_1, x_2) + c_1 x_2] \end{aligned} \quad (28)$$

If the second stabilizing function is selected as

$$\alpha_2(x_1, x_2) = -c_2 z_2 - z_1 - c_1 x_2 \quad (29)$$

then, the derivative of Lyapunov function reduces to

$$\dot{V}_2 = -c_1 z_1^2 - c_2 z_2^2 + z_2 z_3 \quad (30)$$

where $c_2 > 0$ is a design parameter. Still a global stability condition is not satisfied due to $z_2 z_3$ term in the second step.

Step 3.

In the final step, the time-derivative of z_3 is obtained as

$$\dot{z}_3 = \dot{x}_3 - \dot{\alpha}_2(x_1, x_2) \quad (31)$$

Taking the derivative of α_2

$$\dot{\alpha}_2(x_1, x_2) = \frac{\partial \alpha_2}{\partial x_1} \dot{x}_1 + \frac{\partial \alpha_2}{\partial x_2} \dot{x}_2 \quad (32)$$

Equation (31) becomes

$$\dot{z}_3 = a_u f - \frac{\partial \alpha_2}{\partial x_1} x_2 - \frac{\partial \alpha_2}{\partial x_2} x_3 \quad (33)$$

With the increasing number of error variables to (z_1, z_2, z_3) , Lyapunov function is extended as

$$V_3 = V_2 + \frac{1}{2}z_3^2 \quad (34)$$

Continuing the derivation process, one can get

$$\begin{aligned} \dot{V}_3 &= \dot{V}_2 + z_3 \dot{z}_3 \\ &= -c_1 z_1^2 - c_2 z_2^2 + z_2 z_3 \\ &\quad + z_3 \left[a_u f - \frac{\partial \alpha_2}{\partial x_1} x_2 - \frac{\partial \alpha_2}{\partial x_2} x_3 \right] \end{aligned} \quad (35)$$

If the control input f is selected as

$$f = \frac{1}{a_u} \left[-c_3 z_3 - z_2 + \frac{\partial \alpha_2}{\partial x_1} x_2 + \frac{\partial \alpha_2}{\partial x_2} x_3 \right] \quad (36)$$

The time-derivative of V_3 satisfies a global stability such as

$$\dot{V}_3 = -c_1 z_1^2 - c_2 z_2^2 - c_3 z_3^2 < 0 \quad (37)$$

TEST SYSTEM

The vertically designed five axis controlled active magnetic bearing system shown in Figure 4 is used for modeling, simulations and experiments. The AMB system which is manufactured by Koyo Seiko Corporation Ltd., Japan, consist of a CFRP flywheel-AMB, a control unit and a high-frequency inverter. The parameters of the AMB system is given in Table 1.



FIGURE 4: Flywheel-AMB test system

TABLE 1: Parameters of the rotor-AMB system

Symbol	Value(FW)	Unit
M	13.672	kg
I_r	1.73×10^{-1}	kgm^2
I_a	1.86×10^{-1}	kgm^2
L_u	4.99×10^{-2}	m
L_l	1.676×10^{-1}	m
L_1	2.535×10^{-2}	m
L_2	1.8815×10^{-1}	m
K_u	4.47×10^{-6}	Nm^2/A^2
K_l	4.47×10^{-6}	Nm^2/A^2
X_0, Y_0	0.25×10^{-3}	m

EXPERIMENTS

A feedback control system is built with a digital signal processor(DSP) to realize experiments. The control system is a multi-input multi-output structure with four displacements measured by four eddy-current position sensors and eight computed control current signals for actuators. The control current signals for actuators. The control inputs are supplied to electromagnets through D/A converters and power amplifiers.

The trajectories of the geometric center point of the rotor is generally used to evaluate the control performance. The experimental results are presented for near frequencies of the rigid mode of the rotor. The orbits of the rotor obtained at 100 Hz are shown in Figure 5 for lower and upper actuator locations. The control currents in the x direction of the upper and lower electromagnets during the rotational experiment are shown in Figures 6-7. As seen in the figure, only one electromagnet has a current flow at any given time depending on the rotor displacement. For the same system, Figure 8 shows the orbits at 110 Hz rotational speed. Figures 9-10 are control currents for the same rotational speed.

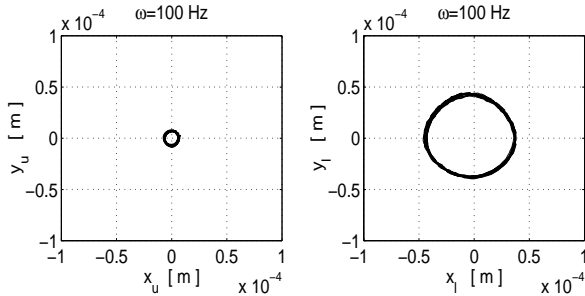


FIGURE 5: Orbit of the rotor for $\omega = 100$ Hz

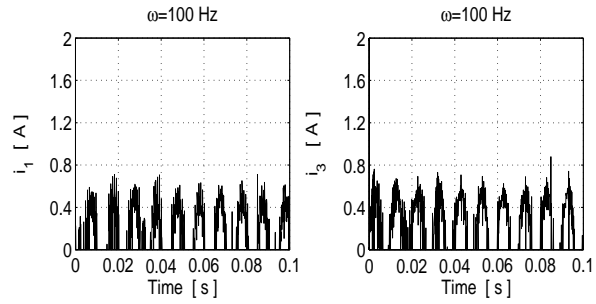


FIGURE 6: Control currents for $\omega = 100$ Hz

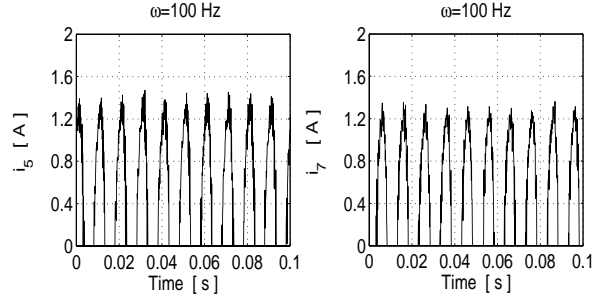


FIGURE 7: Control currents for $\omega = 100$ Hz

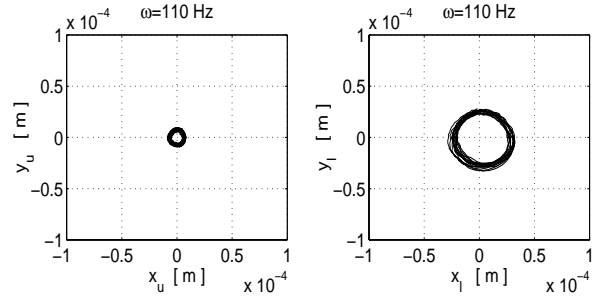


FIGURE 8: Orbit of the rotor for $\omega = 110$ Hz

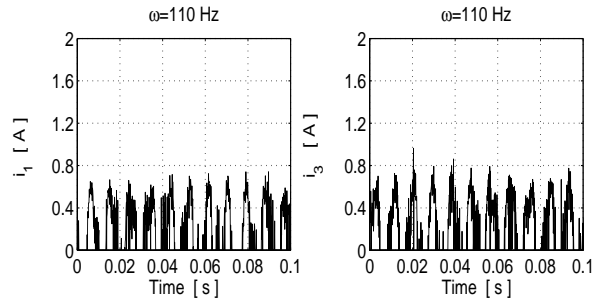


FIGURE 9: Control currents for $\omega = 110$ Hz

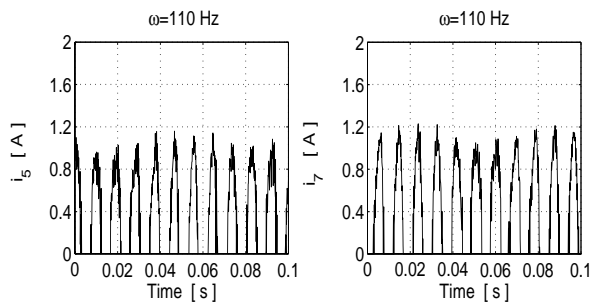


FIGURE 10: Control currents for $\omega = 110$ Hz

CONCLUSIONS

As a research field, zero-bias active magnetic bearings have potential to reduce power consumption and bearing losses. In this research work, a force base switching with a backstepping control approach is successfully applied to a zero bias AMB and obtained reasonable results. In present situation, much research works are needed using different switching rules, power amplifiers and nonlinear control approaches for zero bias AMBs.

References

- [1] G. Schweitzer, "Active Magnetic Bearings-Chances and Limitations," in Proceeding of the 6th International IFToMM Conference on Rotor Dynamics, Sydney, Australia, pp. 1-14, 2002.
- [2] L. Hawkins, E. Blumer, "Development of an AMB Energy Storage Flywheel for Industrial Applications", Proceeding of 7th Int. Symposium on Magnetic Suspension Technology, pp.156-163, Fukuoka, Japan, 2003.
- [3] A. Kubo, H. Kamenno, R. Takahat, S. Gachter, "Dynamic Analysis and Levitation Test in 1kWh class Flywheel Energy Storage System", Proceeding of 7th Int. Symposium on Magnetic Suspension Technology, pp.144-149, Fukuoka, Japan, 2003.
- [4] J. Levine, J. Lottin, J-C. Ponsart: A Non-linear Approach to the Control of Magnetic Bearing, IEEE Transactions on Control System Technology, Vol.4, No.5, pp. 524-544, 1996.
- [5] M.S. Queiroz, D.M. Dawson, *Nonlinear Control of Active Magnetic Bearings: A Backstepping Approach*, IEEE Transactions on Control System Technology, Vol.4, No.5, pp. 545-552, 1996.

- [6] S. Sivrioglu, K. Nonami, "Adaptive Output Backstepping Control of a Flywheel Zero-Power AMB System with Parameter Uncertainty", Proceeding of 42nd IEEE Conference on Decision and Control(CDC), pp.3942-3947, Hawaii-USA, 2003.
- [7] K.Nonami, Z.Liu, "Zero Power Nonlinear Control of Magnetic Bearing System Proceedings of the 8th International Symposium on Magnetic Bearing," pp.83-89, August 26-28, Mito-Japan, 2002.
- [8] K. Sakai, K. Nonami, Y.Ariga: Low Consumption Nonlinear Control of Magnetic Bearing System by means of Backstepping Procedure, Transactions of the Japan Society of Mechanical Engineers (Japanese), vol.67, No. 664, 2001.
- [9] M. Krstic, I. Kanellakopoulos, P. Kokotovic, *Nonlinear and Adaptive Control Design*, John Wiley& Sons, Inc., 1995.
- [10] D.L. Trumper, S.M. Olson, P.K. Subrahmanyam, *Linearizing Control of Magnetic Suspension System*, IEEE Transactions on Control System Technology, Vol.5, No.4, pp. 427-437, 1997.